Precursor evolution and growth mechanism of BTO/YBCO films by TFA–MOD process*

Wang Hong-Yan(王洪艳)[a)b)], Ding Fa-Zhu(丁发柱)[a)†], Gu Hong-Wei(古宏伟)[a)‡], Zhang Teng(张 腾)[a)], and Peng Xing-Yu(彭星煜)[a)b)]

[a)] *Key Laboratory of Applied Superconductivity, Institute of Electrical Engineering, Chinese Academy of Sciences, Beijing* 100190, *China*
[b)] *University of Chinese Academy of Sciences, Beijing* 100049, *China*

(Received 18 February 2014; revised manuscript received 8 April 2014; published online 10 August 2014)

In this study, $BaTiO_3$ (BTO)-doped YBCO films are prepared on $LaAlO_3$ (100) single-crystal substrates by metal–organic decomposition (MOD) using trifluoroacetate (TFA) precursor solutions. The critical current density (J_c) of BTO/YBCO film is as high as 10 MA/cm^2 (77 K, 0 T). The BTO peak is found in the X-ray diffraction (XRD) pattern of a final YBCO superconductivity film. Moreover, a comprehensive study of the precursor evolution is conducted mainly by X-ray analysis and μ-Raman spectroscopy. It is found that the TFA begins to decompose at the beginning of the thermal process, and then further decomposes as temperature increases, and at 700 °C BTO nanoparticles begin to appear. It suggests that the YBCO film embedded with BTO nanoparticles, whose critical current density (J_c) is enhanced, is successfully prepared by an easily scalable chemical solution deposition technique.

Keywords: $YBa_2Cu_3O_{7-x}$, precursor evolution, $BaTiO_3$, TFA–MOD

PACS: 74.78.–w, 81.16.Dn **DOI:** 10.1088/1674-1056/23/10/107402

1. Introduction

$YBa_2Cu_3O_{7-x}$ (YBCO) coated conductors, which are high current conductors that display outstanding performances in the respect of temperature and magnetic field, are the most promising materials for power systems and magnets. In recent years, YBCO coated conductors have been the subject of considerable research efforts and many great breakthroughs have been achieved. Early in 2009, Superpower Inc.[1] routinely fabricated 10^3-m YBCO tapes with a minimum critical current ($I_{c)}$ of about 300 A/cm-w. In 2011, Fujikura Ltd.[2] succeeded in over 800-m long Y-based coated conductors with the uniform I_c 572 A/cm-w. In 2013, AMSC[3] prepared a 1.2-μm YBCO film, whose I_c reached 500 A/cm-w in production length. The power applications of superconductors will be tremendously increased if the YBCO tapes can carry 10^3 amperes in 1-cm width, which is also the benchmark of US Department of Energy, and therefore the value of I_c represents the efforts of fundamental research of YBCO.[4,5] There is a direct correlation between I_c and J_c: increasing J_c means being able to carry a higher current within the same wire. At present, the critical strategies to enhance J_c mainly include substrate surface decoration,[6–9] impurity addition,[10–13] Rare earth (RE) addition or substitution,[14–18] and combined methods.[19,20] Among these strategies, the enhancement of J_c in YBCO film based on impurity addition is attractive because it is a simple, practical, and scalable route for both better performance and lower fabrication cost. In 2004, $BaZrO_3$ (BZO), an epitaxial second phase, was introduced into YBCO film to improve J_c for the first time by pulsed laser deposition (PLD),[21] which led to a 1.5-5-fold improvement in the in-magnetic-field current density of the conductor, which is already of high quality. In 2007, Gutierrez *et al.*[22] prepared BZO/YBCO film by metal–organic decomposition (MOD) of trifluoroacetate (TFA) process, which was also very effective in enhancing the value of J_c.

TFA–MOD has been demonstrated to be a very promising technique for the large-scale production of coated conductors (CCs) because it does not require any expensive vacuum apparatus and it could prepare a high-J_c YBCO layer from the TFA precursor. However, the complex reaction process of TFA–MOD requires precisely controlled parameters to achieve high performance YBCO films.[23] Araki and Hirabayashi[24] discussed all the TFA–MOD processes and the peculiar growth scheme of the YBCO layer in TFA–MOD. Gazquez *et al.*[25] reported a microstructural analysis of the conversion process of Y, Ba, and Cu TFA precursors to epitaxial YBCO films after the pyrolysis step. Zalamova *et al.*[26] studied the mechanisms of controlling stress relief during the drying and pyrolysis of trifluoroacetate metal–organic precursors. Llordes *et al.*[27] determined the complete decomposition reaction by the released gases during metal–trifluoroacetate thermal decomposition. Although the chemical reaction path prior to high performance pure YBCO nucleation has been extensively studied, many details of the process are still unclear. Especially

*Project supported by the National Natural Science Foundation of China (Grant Nos. 51002149 and 51272250) and the National Basic Research Program of China (Grant No. 2011CBA00105).

†Corresponding author. E-mail: dingfazhu@mail.iee.ac.cn
‡Corresponding author. E-mail: guhw@mail.iee.ac.cn

© 2014 Chinese Physical Society and IOP Publishing Ltd

when high performance YBCO films are prepared by impurity addition using TFA–MOD process, the precursor evolution of nanoparticles of this process is still an open question. The knowledge of the precursor evolution is essential for the YBCO coated conductors with competitive superconducting performance.

In this work, YBCO superconductor films with BTO additions were successfully prepared by a TFA–MOD process, whose J_c can reach 10 MA/cm^2 (77 K, 0 T). We also carry out a thorough and analytical study of both solid decomposition remnants and their nucleation process of BTO/YBCO precursor gel. Finally, a preliminary analysis of the growth mechanism of BTO/YBCO is performed and the reasons for enhancing the performance of YBCO films are discussed.

2. Experimental methods

With TFA–MOD process, we prepared superconducting YBCO films by using complex metal–organic solutions for epitaxial BTO/YBCO film, including the acetates of yttrium, barium and copper and Ti acetylacetonate (TiAcAc) precursors in stoichiometric proportions. The molar content of BTO in the investigated BTO/YBCO nanocomposite was about 6% and the concentration of the TFA solution was 1.5 M. The additional acetate of barium was added to compensate for the barium loss in YBCO and the moles ratio of the additional barium and Ti acetylacetonate was 1:1. Solution deposition was carried out for 1 min by spin coating on 10 mm×10 mm (00l)-oriented $LaAlO_3$ single-crystal substrates at 3000 rpm (1 rpm = 1 r/min). Then, the samples were immediately placed in a quartz tube within a horizontal furnace. The coated films were calcined at the temperature up to 400 °C in 4.2% humidified oxygen. Then, the calcined films were calcined at 820 °C in humidified Ar gas mixed with oxygen gas and finally oxygenated at 500 °C for 90 min in oxygen. The analysis of intermediate phase was taken by quenching at different temperatures. We prepared many precursor films coated on $(00l)$-oriented $LaAlO_3$ single-crystal substrates, which were placed in a tubular furnace and heated to 200 °C, 300 °C, 500 °C, 700 °C, and 750 °C, respectively, at a heating rate of 300 °C/h in humidified oxygen, and then kept 100 min at a corresponding temperature. Finally, the samples were quenched quickly by taking them out of the furnace and they were cooled down to room temperature

The film thickness was determined to be ∼ 200 nm by profilometer analysis. The surface morphologies of YBCO films were observed by field emission scanning electron microscopy (FESEM, FEI-Siron) equipped with energy-dispersive X-ray spectrometer (EDS). The phase and texture of the as-grown film were characterized by X-ray diffraction (XRD) using Cu-Kα radiation (Bruker D8 Focus) and Raman analysis. μ-Raman measurements were carried out using the 532-nm line of an argon–ion laser at room temperature with an inVia-Reflex Raman spectrometer. All of the Raman spectra were recorded at ambient temperature. The thermal decomposition pathway of TFA precursor solution was examined by means of thermogravimetric analysis (TGA) (TA Instruments TGA Q50) in air at 20 °C/min at temperatures increasing from room temperature up to 900 °C. The J_c was measured by J_c-scan Leipzig system.

3. Results and discussion

The performances of YBCO films are tremendously enhanced by introducing nanoparticles into YBCO films. Here, the critical current density (J_c) is achieved to be 10 MA/cm^2 (77 K, 0 T, about 200 nm) by introducing BTO in YBCO films, which are prepared on LAO (001) substrate at a calcining temperature of 820 °C. Figure 1 shows the J_c map measured by J_c-Scan Lepizig system. Currently, the best 0.2-μm thick YBCO films have J_c values on the order of 6.5 MA/cm^2–10 MA/cm^2.[15,18] It is worth mentioning that Gutierrez *et al.* achieved 6.5 MA/cm^2 (77 K, 0 T) and ∼ 11 MA/cm^2 (65 K, 0 T) in 0.2-μm-thick YBCO films with BZO addition by TFA–MOD, which were published in Nature Materials in 2007.[22] In the present paper, our J_c value of BTO/YBCO film is close to these values.

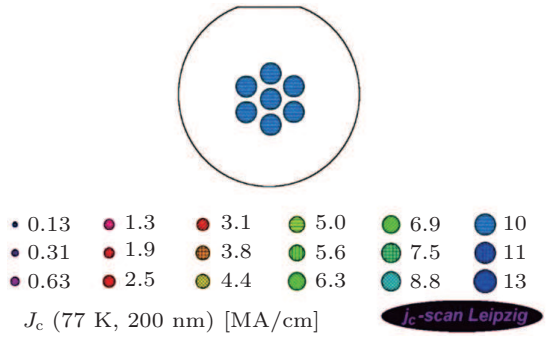


Fig. 1. (color online) J_c mapping over 2-in (1 in = 2.54 cm) area for YBCO films.

Figure 2 shows the XRD θ–2θ Bragg profiles of the BTO/YBCO film prepared at a calcining temperature of 820 °C. It can be seen that all of the major diffraction peaks correspond to the (00l) YBCO peaks, which indicates a well-textured, c-axis oriented YBCO grain structure. Moreover, there are three weak peaks that may be assigned to BTO and some other weak peaks that are assigned to Y_2O_3 and BaF_2, their forming process will be studied in more detail later on in this paper in detail. It can be clearly seen that the two peaks at 2θ angles of 41.108° and 44.961° from the BTO-doped YBCO film can be indexed to the BTO (203) and (200), respectively, which is the direct evidence for the formation of BTO phases in the YBCO film. The relatively weak intensities of BTO peaks are due to the small fraction of BTO, small BZO particle size, and random BZO orientation. We can infer from above descriptions that BTO nanoparticles are indeed formed in the

BTO-doped YBCO film under the same growth conditions as in YBCO films.

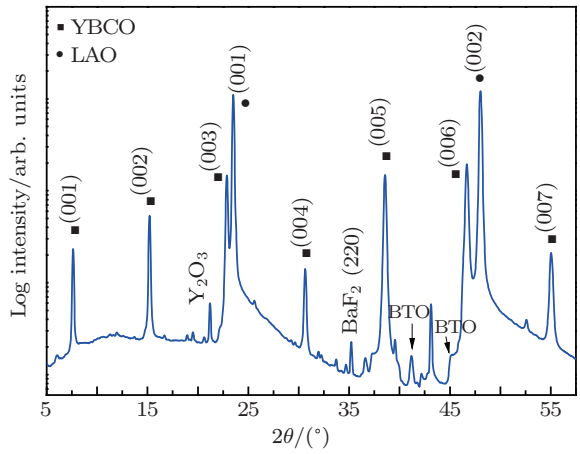


Fig. 2. (color online) XRD θ–2θ pattern of YBCO-6 mol% BTO composite film grown on (100) $LaAlO_3$.

Apparently, the final YBCO films prepared from complex metal–organic solutions added with TiAcAc exhibit the high performances. It is important to understand the precursor evolution and growth mechanism of BTO/YBCO film by TFA–MOD process. TGA-DTA analysis allows the first knowledge of that process to investigate the details of the endothermic drying process and the exothermic pyrolysis process occurring in the process of $BaTiO_3$-doped YBCO by the TFA–MOD method. Early works[24–27] have suggested that TFA precursors for YBCO growth decompose mainly in a temperature range 250 °C–320 °C, and some weight loss is already detected below 250 °C. In the present paper, TGA-DTG (Fig. 3) reveals that the decomposition process proceeds, which is similar to what was described in the previous works. The weight is mainly lost at temperatures ranging from 250 °C to 350 °C, which was caused by expelling the residue.[24,27] The weight loss in a temperature range from the room temperature to 250 °C may be caused by both the dehydration and evaporation of the organic solvent, and also by metal trifluoroacetate decomposition.

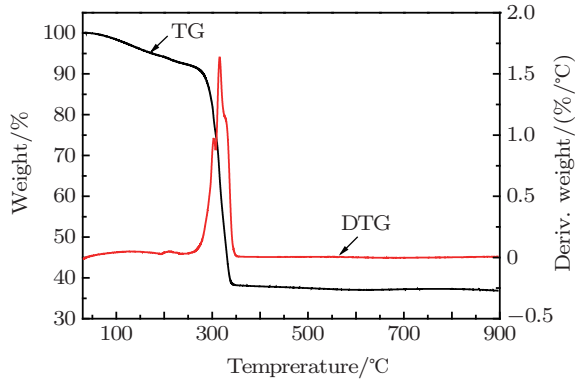


Fig. 3. (color online) TG/DTG record of an anhydrous BTO precursor (10 °C/min).

The precursor films at different quenched temperatures are used to clarify the process of these second phases in Fig. 2. Figure 4 shows the XRD patterns of the YBCO precursor films of different thermal treatments. It can be seen that trifluoroacetic acid salt (TFAS) decomposed at 200 °C and formed some weak peaks, which are associated with Y_2O_3, CuO, BaO, BaF_2 (Ba(O, F)), and YF_3. With the increasing of quenched temperature, the XRD intensities of Y_2O_3, CuO, (Ba(O, F), and YF_3 weaken gradually. Two diffraction peaks of TiO_2 appear at 700 °C. Meanwhile the BTO (203) diffraction peak appears at 700 °C, and the BTO (110) diffraction peak occurs at 750 °C. At the same time, the YBCO peaks appear at 750 °C, and all the peaks of the *c*-axis-oriented YBCO grain occur at 770 °C. To clarify this process, we performed a Raman spectrometry study to identify the intermediate phases. Figure 5 shows μ-Raman spectra measured at pyrolysis temperatures of 300 °C, 500 °C, 750 °C, 770 °C, and 820 °C respectively. The peak at ~ 515 cm^{-1} appears at 750 °C, which is attributed to A1(TO) due to BTO and TiO_2 nanoparticle.[28,29] Accordingly, the peaks at ~ 337 cm^{-1}, ~ 495 cm^{-1}, ~ 565 cm^{-1}, and ~ 622 cm^{-1} are assigned to YBCO,[30,31] and the peak at ~ 622 cm^{-1}, which is assigned to the Cu–O stretching vibration of YBCO, is the typical peak of orthorhombic YBCO, this indicates the formation of a relatively complete structure of copper and oxygen. The Raman scattering peaks imply that the YBCO presents relatively good crystallinity. All of these Raman analyses are in good agreement with the analyses above, which further confirms the existence of intermediate or segregated phase TiO_2.

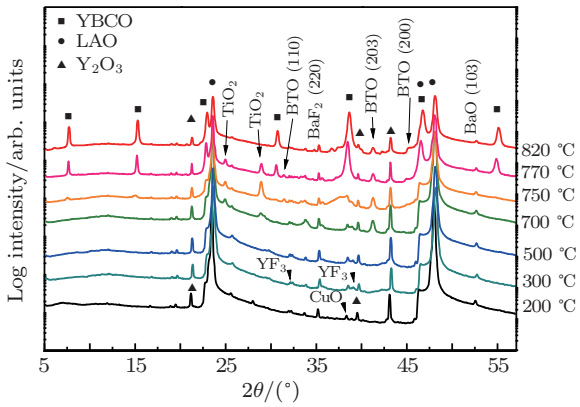


Fig. 4. (color online) XRD θ–2θ patterns of YBCO-6 mol% BTO composite film grown on (100) $LaAlO_3$ for several different quenching temperatures.

From the present results, the reaction path for BTO/YBCO formation can be defined. XRD and Raman analysis reveal that TFAS begins to decompose at 200 °C, and forms the pyrolysis precursor film with a mixture of Y_2O_3, CuO, Ba(O, F), and YF_3. The expected chemical reaction for this process can be written as follows. Upon raising the quenching temperature toward 700 °C, the TiO_2 and the BTO diffraction peaks appear, which means that the TiAcAc begins to pyrolysis and gives out residual gases. We can attribute the small content of TiAcAc to the unchanged weight of the TGA/DTG. Subsequently, TiO_2 reacts with BaO and

finally $BaTiO_3$ is formed, and then the possible chemical reaction for this decomposition step will take place. It can be seen from Fig. 4 that all of the (00l) $YBa_2Cu_3O_{7-x}$ peaks appear at 750 °C and displace some second phases, which means that the intermediate phases begin to transform into the $YBa_2Cu_3O_{7-x}$. Finally, we should note that the XRD diffraction peaks of TiO_2 disappear at 820 °C, and a few of the BTO peaks and all the *c*-axis oriented YBCO peaks remain, which suggests that the TiO_2 changes into BTO completely and the BTO nanoparticles can form under the same growth conditions as those for YBCO films.

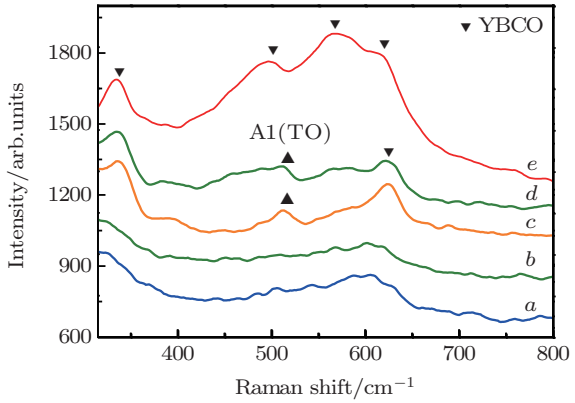


Fig. 5. (color online) Raman spectra of YBCO-6 mol% BTO films intermediate phase for different quenching temperatures: 300 °C (curve *a*), 500 °C (curve *b*), 750 °C (curve *c*), 770 °C (curve *d*), and 820 °C (curve *e*).

$$(CF_3COO)_3Y + (CF_3COO)_2Ba + (CF_3COO)_2Cu + H_2O \xrightarrow{200\ ^\circ C} Y_2O_3 + Ba(O, F) + CuO + YF_3 + CO_2\uparrow, \quad (a)$$

$$C_{10}H_{14}O_5Ti + O_2 \xrightarrow{700\ ^\circ C} TiO_2 + H_2O\uparrow + CO_2\uparrow, \quad (b)$$

$$TiO_2 + BaO \xrightarrow{700\ ^\circ C} BaTiO_3, \quad (c)$$

$$Ba(O, F) + CuO + Y_2O_3 + H_2O \xrightarrow[O_2]{750\ ^\circ C} YBa_2Cu_3O_{7-x} + HF\uparrow. \quad (d)$$

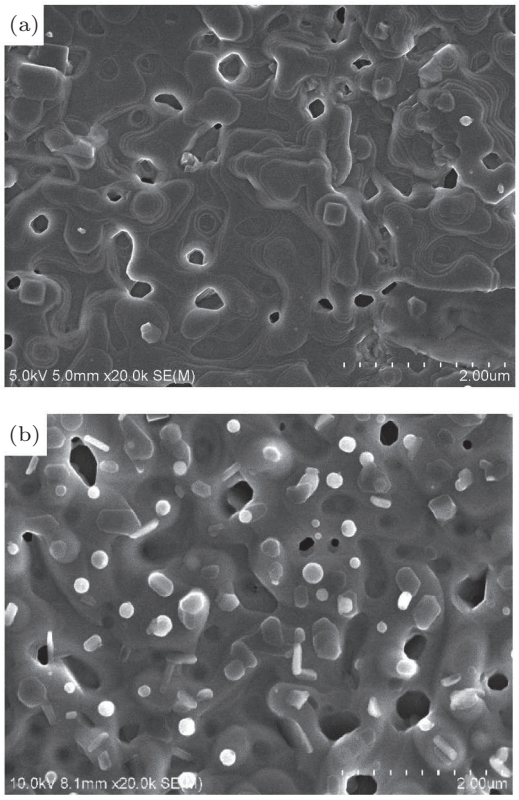


Fig. 6. SEM micrographs of (a) pure YBCO film and (b) YBCO-6%mol BTO film.

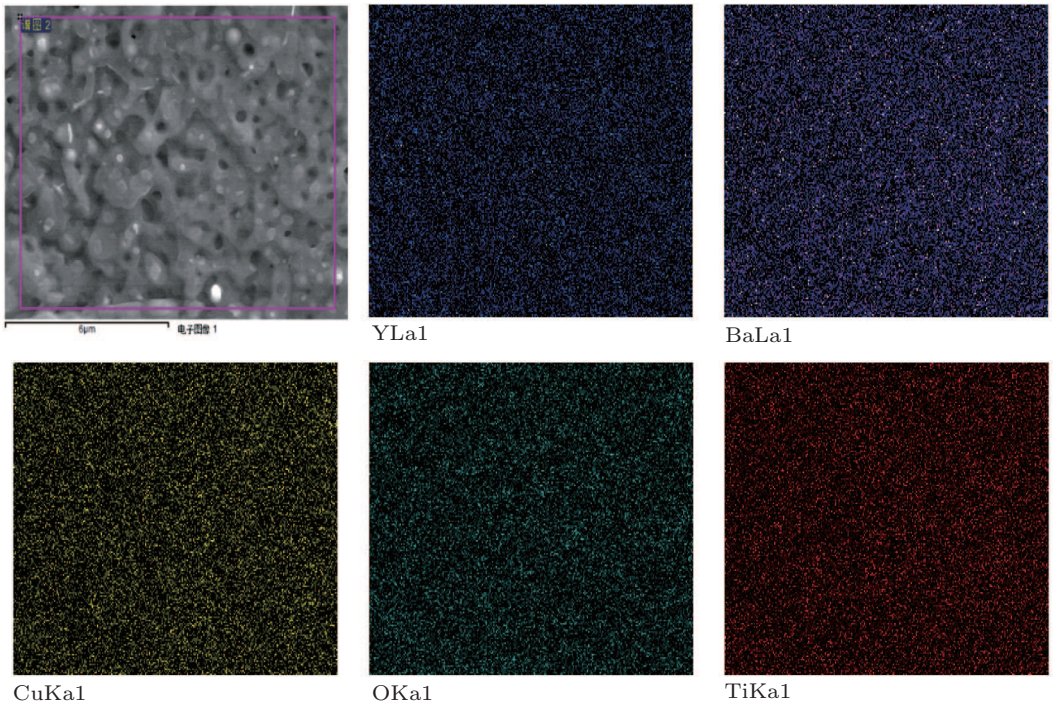


Fig. 7. (color online) EDS maps of Y, Ba, Cu, O, Ti elements on the surfaces of YBCO-6%-mol BTO films.

Figure 6 shows the typical SEM micrographs of the pure YBCO film and the BTO/YBCO film. The surface morphologies we can observe from both samples are smooth in density and crack-free. In addition, many nanoparticles (the bright points) and solid holes can be found on the surface of BTO-doped YBCO film, which is different from the scenario of pure YBCO graph. These nanoparticles are randomly scattered across the film surface, and the dimensions of the particles in the BTO/YBCO film are in the dozens of nanometers. Based on the above analyses, these nanoparticles and solid holes are probably of the BTO phase because the crystallization of BTO in the YBCO film is complete after thermal annealing at 820 °C (see Fig. 4). The compositions of these particles are confirmed by EDS spectra. It is observed from Fig. 7 that the nanoparticles in the film have a high Ti content. In addition, the distributions of titanium is uniform rather than clustered together.

4. Summary

In this study, we prepared BTO/YBCO superconducting films by TFA–MOD process, which leads to a great enhancement of J_c (10 MA/cm^2@77 K, 0 T). The reaction path for BTO/YBCO formation is determined by XRD and Raman analysis. We find that the trifluoroacetic acid salt (TFAS) is decomposed at 200 °C and forms Y_2O_3, CuO, Ba(O, F), and YF_3. The crystalline phase of BTO nanoparticles appears at 700 °C and TiO_2 forms at the same temperature. When the temperature rises to 820 °C, the TiO_2 disappears and BTO diffraction remains there, which probably results in the enhancement of J_c.

References

[1] Lehner T F, 2G HTS Wire status in the USA, 2011, available at http://www.superpower-inc.com/system/files/2011_1031+ISIS20_Korea_US+2G+HTS+Wire+Update_TL.pdf

[2] Daibo M, Kakimoto K, Kikutake R, Suzuki R, Lijima Y, Itoh M and Saitoh T 2011 *Fujikura Technical Report* **2** 121

[3] Rupich M W, Li X P, Sathyamurthy S, Thieme C L H, DeMoranville K, Gannon J and Fleshler S 2013 *IEEE T. Appl. Supercond.* **23** 6601205

[4] Foltyn S R, Wang H, Civale L, Jia Q X and Arendt P N 2005 *Appl. Phys. Lett.* **87** 162505

[5] Feldmann D M, Holesinger T G, Maiorov B, Zhou H, Foltyn S R, Coulter J Y and Apodoca I 2010 *Supercond. Sci. Technol.* **23** 115016

[6] Crisan A, Fujiwara S, Nie J C, Sundaresan A and Ihara H 2001 *Appl. Phys. Lett.* **79** 4547

[7] Maiorov B, Wang H, Foltyn S R, Li Y, DePaula R, Stan L, Arendt P N and Civale L 2006 *Supercond. Sci. Technol.* **19** 891

[8] Aytug T, Paranthaman M, Gapud A A, Kang S, Christen H M, Leonard K J, Martin P M, Thompson J R, Christen D K, Meng R, Rusakova I, Chu C W and Johansen T 2005 *J. Appl. Phys.* **98** 114309

[9] Öztürka A, Düzgünb I and Elebi S C 2010 *J. Alloys Compd.* **795** 104

[10] Lu F, Kametani F and Hellstrom E E 2013 *Supercond. Sci. Technol.* **26** 045016

[11] Emergo R L S, Baca F J, Wu J Z, Haugan T J and Barnes P N 2010 *Supercond. Sci. Technol.* **23** 115010

[12] Maiorov B, Baily S A, Zhou H, Ugurlu O, Kennison J A, Dowden P C, Holesinger T G, Foltyn S R and Civale L 2009 *Nat. Mater.* **8** 398

[13] Ding F Z, Gu H W, Zhang T, Wang H Y, Qu F, Qiu Q Q, Dai S T and Peng X Y 2013 *Chin. Phys. B* **22** 077401

[14] Cai B, Holzapfel B, Hanisch J, Fernandez L and Schultz L 2004 *Phys. Rev. B* **69** 104531

[15] MacManus-Driscoll J L, Foltyn S R, Maiorov B, Jia Q X, Wang H, Serquls A, Civale L, Lin Y, Hawley M E, Maley M P and Peterson D E 2005 *Appl. Phys. Lett.* **86** 032505

[16] Develos-Bagarinao K and Yamasaki H 2011 *Supercond. Sci. Technol.* **24** 065017

[17] Yamada Y, Takahashi K, Kobayashi H, Konishi M, Watanabe T, Ibi A, Muroga T, Miyata S, Kato T, Hirayama T and Shiohara Y 2005 *Appl. Phys. Lett.* **87** 132502

[18] Nakaoka K, Matsuda J, Kitoh Y, Goto T, Yamada Y, Izumi T and Shiohara Y 2007 *Physica C* **519** 463

[19] Chen Y Q, Yan F Y, You C Y, Zhao G Y and Jiao Y 2013 *J. Alloys Compd.* **576** 265

[20] Kang S, Leonard K J, Martin P M, Li J and Goyal A 2007 *Supercond. Sci. Technol.* **20** 11

[21] MacManus-Driscoll J L, Foltyn S R, Jia Q X, Wang H, Serquis A and Civale L 2004 *Nat. Mater.* **3** 439

[22] Gutierrez J, Llordes A, Gazquez J, Gibert M, Roma N and Ricart S 2007 *Nat. Mater.* **6** 367

[23] Ding F Z, Lu X D, Gu H W, Li T and Cao J L 2009 *Chin. Phys. B* **18** 1631

[24] Araki T and Hirabayashi I 2003 *Supercond. Sci. Technol.* **16** R71

[25] Gazquez J, Sandiumenge F, Coll M, Pomar A, Mestres N, Puig T, Obradors X, Kihn Y, Casanove M J and Ballesteros C 2006 *Chem. Mater.* **18** 6211

[26] Zalamova K, Roma N, Pomar A, Morlens S, Puig T, Gazquez J, Carrillo A E, Sandiumenge F, Ricart S, Mestres N and Obradors X 2006 *Chem. Mater.* **18** 5897

[27] Llordeés A, Zalamova K, Ricart S, Palau A, Pomar A and Puig T 2010 *Chem. Mater.* **22** 1686

[28] Garcia-Hernandez M, Chadeyron G, Boyer D, Garcia-Murillo A, Carrillo-Romo F and Mahiou R 2013 *Nano Micro. Lett.* **5** 57

[29] Zhang Y H, Chan C K, Porter J F and Guo W 1998 *J. Mater. Res.* **13** 2602

[30] Maroni V A, Li Y, Feldmann D M and Jia Q X 2007 *J. Appl. Phys.* **102** 113909

[31] Maroni V A, Reeves J L and Schwab G 2007 *Appl. Spectrosc.* **61** 359